Spatio-temporal analysis of land surface temperature in Siddharthanagar (1993–2024)

Prashamsa Shrestha [*] and Neel Kamal Koju [**]

[*]Naaya Aayam Multi-Disciplinary Institute (NAMI), University of Northampton, Baneshwor, 44600 Kathmandu, Nepal.

[**]Nepal Academy of Science and Technology, Khumaltar, Lalitpur, Nepal.

Abstract: Land Surface Temperature (LST) refers to the radiative temperature of the Earth's surface, as measured by satellite sensors. This study employs Remote Sensing technologies to conduct a detailed spatio-temporal analysis of LST trends in Siddharthanagar from 1993 to 2024. The research focuses on analyzing temporal LST patterns, investigating the spatial distribution, and examining the factors influencing LST, particularly Land Use Land Cover (LULC) and the Normalized Difference Vegetation Index (NDVI). Using Landsat-5 and Landsat-8 satellite data processed through Google Earth Engine (GEE), LST values were derived from thermal bands. The results show a significant rise in LST, with an average annual increase of 0.18°C. Areas with dense vegetation, indicated by higher NDVI values, have lower LST, while regions with sparse vegetation such as bare ground and range lands experience higher LST. The study highlights the critical role of vegetation in regulating surface temperatures and the need for sustainable urban planning to mitigate rising temperatures and the Urban Heat Island (UHI) effect.

Keywords: Land surface temperature; Land use; Land cover; NDVI; Remote sensing; Urban heat Island.

Introduction

Land Surface Temperature (LST) is a fundamental geophysical parameter that evaluates the global surface characteristics such as water and energy balance in the land-atmosphere system. LST datasets provide crucial information for measuring global environmental changes and their impacts on climate [1, 2] with applications in surface evaporation estimation, surface energy balance, and monitoring surface heat effects [3, 4]. LST varies across spatial and temporal scales, making it a key indicator for assessing land-use and land-cover (LULC) changes and exploring the urban heat island (UHI) effect [5, 6, 7]. Remote sensing and Geographic Information System (GIS) technologies have become the primary tools for monitoring spatiotemporal LST dynamics, with thermal infrared satellite imagery enabling consistent, long-term assessment of urban surface temperatures and their relationship with LULC change, supporting evidence-based environmental planning [8, 9].

Globally, LST has been rising with rapid urbanization, which replaces blue-green and permeable surfaces with impervious built-up areas such as buildings and roads. This transformation intensifies the UHI effect, elevating energy consumption, degrading air quality, and amplifying heat-related health risks [10, 11]. Major South Asian cities, including Mumbai, Kolkata, Delhi, and Karachi, have already experienced significant increases in LST and associated heat-wave mortality [8,12]. As global temperatures continue to rise, the World Health Organization identifies heat waves among the most dangerous natural hazards, with South Asia projected to face increasingly frequent and severe humid heat events [13].

In Nepal, urbanization has accelerated markedly, with urban areas growing at 5.3% annually, driven by rural-to-urban migration, population growth, and administrative reclassification [14]. Expansion has been most pronounced in

Author for correspondence: Neel Kamal Koju, Nepal Academy of Science and Technology, Khumaltar, Lalitpur, Nepal.
Email: neelkamalkoju@gmail.com; https://orchid.org/0000-0003-2000-4431
Received: 26 Apr, 2026; Received in revised form: 31 May, 2026; Accepted: 7 Jun, 2026.
Doi: https://doi.org/10.3126/sw.v19i19.95719

the Tarai and mid-Hills regions, where natural land cover and agricultural land have been progressively replaced by built-up areas, directly contributing to rising LST across Nepali urban centers [15, 16]. For instance, in Nepalgunj, vegetation declined while bare land and human structures expanded considerably between 1996 and 2020 [17]. The Normalized Difference Vegetation Index (NDVI), which reflects vegetation cover, is negatively correlated with LST; as urban areas expand and green cover diminishes, surface temperatures correspondingly rise, further intensifying local UHI conditions [18, 19].

Siddharthanagar Municipality, located in the Tarai lowlands of Nepal, exemplifies these pressures. Its population has grown from 39,473 in 1991 to 76,307 in 2021, with projections reaching 133,028 by 2030 [20, 21,14]. Vegetation and water bodies, which provide a natural cooling effect, account for only 0.12% and 0.87% of the municipality's land cover, respectively, while barren land covers 12.65%, contributing to elevated LST [22]. The city already experiences extreme heat, with air temperatures reaching up to 43°C, resulting in a growing number of heat-related hospitalizations at Lumbini Provincial Hospital [13].

Yet despite this acute and growing heat burden, Siddharthanagar has received no dedicated LST study. While global research on LST is extensive with China leading in published studies [23], Nepal's contribution remains limited. Existing studies have focused primarily on larger urban centers such as Kathmandu and Nepalgunj, leaving a significant gap at the local level for rapidly urbanizing Tarai municipalities where heat stress is most severe and the need for targeted mitigation strategies is most urgent.

This study therefore aims to conduct a comprehensive temporal and spatial analysis of LST trends in Siddharthanagar from 1993 to 2024 using GIS and remote sensing. The specific objectives are: (i) to analyze the temporal trends of LST over the study period; (ii) to investigate the spatial distribution and variation of LST across the municipality; and (iii) to identify the key factors influencing LST dynamics.

The study was subject to several limitations. The low spatial resolution of available satellite imagery and the absence of adequate in-situ meteorological data constrained the validation of satellite-derived LST. Cloud cover presented a further challenge, as thermal infrared sensors cannot penetrate clouds, resulting in data gaps and preventing a consistent temporal sampling interval throughout the study period.

Siddharthanagar (formerly Bhairawa) is located in Rupandehi District, Lumbini Province, in the southwestern Tarai region of Nepal, bordering India (Figure 1). Established as Bhairahawa Nagar Panchayat in 1967 A.D. and renamed in 1976 A.D. to honor Siddhartha Gautama, the municipality spans 36.03 km² across 13 wards at 83°26' E and 27°31' N, with a population of 76,307 as of 2021 [21,24]. The city serves as a major administrative, commercial, and transit hub between Nepal and India, and its proximity to Lumbini a UNESCO World Heritage Site makes it a significant tourist centre, receiving 16.7% of Nepal's tourists in 2017 [25]. Siddharthanagar has a hot and humid tropical climate with a biologically diverse floodplain. Land use is dominated by agriculture (77.74%), primarily maize, millet, and wheat, while forest cover accounts for just 0.12% of the area [22]. Rapid urbanization, accelerated by the construction of a national highway and Gautam Buddha International Airport, has intensified pressure on natural habitats and contributed to the environmental challenges the city now faces [26].

The LULC map 2023 is categorized into six classes: water bodies, tree cover, cropland, built-up areas, bare ground, and rangeland as shown in Figure 2. The most significant observation is the dominance of the built-up regions, marked in red, which covers a substantial portion of Siddharthanagar, especially in the northern and central wards such as Ward 8 and Ward 6. The cropland, indicated in orange, appears to be prevalent in southern and western regions, particularly in Ward 10 and Ward 2. Small patches of trees (green) and water bodies (blue) are scattered across the region. The presence of rangeland, marked in light yellow, is sparsely distributed, with some coverage in the western part (Ward 11).

Methodology

Study area

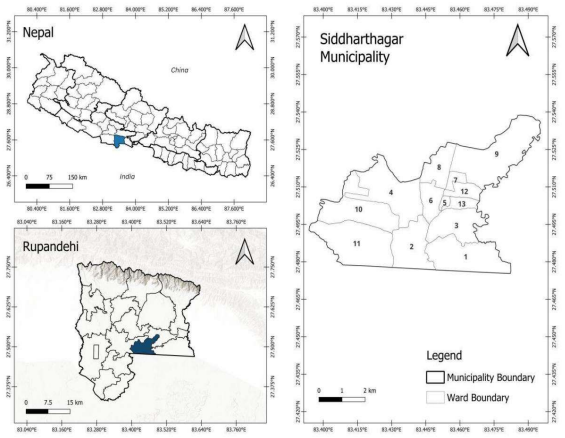

Figure 1: Study site map of Siddharthanagar Municipality.

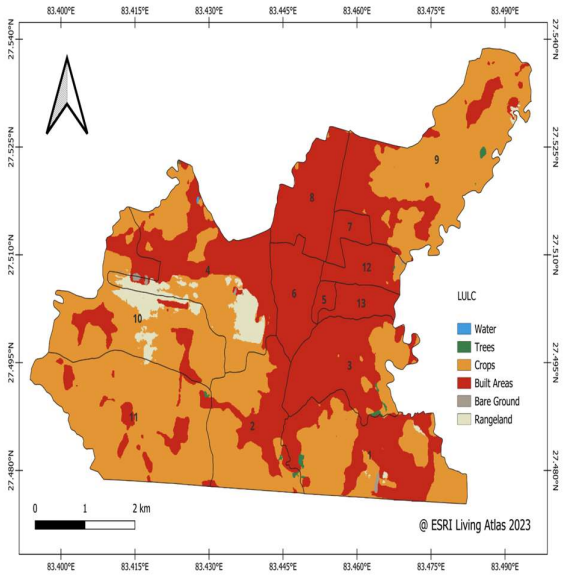

Figure 2: LULC map of Siddharthanagar in 2023.

The LULC map 2023 is categorized into six classes: water bodies, tree cover, cropland, built-up areas, bare ground, and rangeland as shown in Figure 2. The most significant observation is the dominance of the built-up regions, marked in red, which covers a substantial portion of Siddharthanagar, especially in the northern and central wards such as Ward 8 and Ward 6. The cropland, indicated in orange, appears to be prevalent in southern and western regions, particularly in Ward 10 and Ward 2. Small patches of trees (green) and water bodies (blue) are scattered across the region. The presence of rangeland, marked in light yellow, is sparsely distributed, with some coverage in the western part (Ward 11).

Data Acquisition

In the first phase, data acquisition was conducted using the Google Earth Engine (GEE) platform, a cloud-computing environment that provides access to large-scale geospatial datasets. Landsat-5 Thematic Mapper (TM) Tier-1 Surface Reflectance (SR) data were used for years prior to 2012, while Landsat-8 Operational Land Imager (OLI) and TIRS Tier-1 SR data were used for 2012 onwards [27]. For each study year, imagery was filtered to the pre-monsoon months of March to May, as this period captures the peak heat stress season in Nepal, when heatwaves are most frequently observed [16]. LST values were then averaged across these three months to produce a single mean LST representative of the pre-monsoon season for each study year. This acquisition and averaging procedure were applied for the years 1992, 1996, 2004, 2008, 2011, 2014, 2018, 2022, and 2024. All imagery was filtered for cloud cover below 10% and screened using quality assurance bands to ensure data reliability.

Data Preparation

Following data acquisition, the satellite imagery was clipped to the study area boundary using a municipal shapefile to spatially constrain the analysis. Vector datasets containing provincial and district boundaries and road network data were additionally integrated into the GEE workspace to support spatial referencing and visualization. Monthly SR composites for March, April, and May were averaged for each study year to produce a single pre-monsoon mean image per year, following the approach of Li et al. (2020), who applied an equivalent averaging procedure for Landsat-5 and Landsat-8 Top of Atmosphere (TOA) data. These averaged images were subsequently used as the basis for LST retrieval and LULC classification. The acquisition dates and associated metadata for each Landsat scene are provided in Appendix 3.

Retrieving LST

LST retrieval is conducted using a detailed work - flow

shown in Figure 3 with Landsat 5 Collection-2, Level-2 data, Landsat 8 Collection-2, Level-2 data and GEE. The pre-processed images went under atmospheric and radiometric corrections and were then filtered based on specific parameters, such as the year range, months, and cloud cover. To maintain the quality of the data, cloud and cloud shadow masking techniques are applied. A scaling factor is used to convert the thermal bands to surface temperature (ST) in Celsius, resulting in a processed image collection, as adapted from Waleed et al. (2021).

For LST estimation, data from the OLI, particularly SR bands 4 and 5, are used to compute the NDVI. This index determines vegetation density, which is essential for calculating land surface emissivity. Landsat-5 TM has one thermal band (band 6) but for Landsat 8, TOA images and brightness temperature values from band 10 are employed in the LST retrieval process. Band 11 of the TIRS is excluded due to calibration challenges, following the guidelines of the United States Geological Survey. After processing the images, LST is calculated using the equation (i) provided below. The full procedure, along with all relevant equations, is detailed in Appendix 1. This methodology ensures accurate LST extraction from Landsat 5/8 data over the selected period, with the extraction code provided in Appendix 2 as adapted from Waleed et al. (2021).

$$S_T = \frac{T_B}{1+\left(\frac{\lambda \times T_B}{\rho}\right)\times \ln \varepsilon} - 273.15 \text{…….(i)}$$

where,

S_T = LST in (°C),

T_B = at-satellite brightness temperature (K),

λ = wavelength of emitted radiance (11.5 μm),

ρ = 1.438 × 10−2 mK,

ε = emissivity (ranges from 0.97 to 0.99).

Results and Discussion

1. Temporal Trend of LST

The LST values in Siddharthanagar have fluctuated over thestudy period but show a clear upward trend overall (figure 4). The mean LST increased from 35.93°C in 1993 to 41.52°C in 2024, representing an average annual rise of approximately 0.18°C over 31 years. The highest maximum temperature of 47.87°C was recorded in 2024, compared to 41.40°C in 1993 — an increase of over 6°C in thredecades. The most significant peaks in mean LST occurred in 2008 (42.16°C) and 2022 (41.98°C), indicating increasingly frequent extreme heat periods. The only notable cooling period occurred in 2004, when both the minimum (29.82°C) and maximum (39.80°C) LST values were the lowest recorded across the entire study period. Full annual LST statistics are provided in Appendix 4.

The rising trend is primarily driven by rapid urbanization, reduced vegetation cover, and broader climatic changes. The city's population, projected to reach 133,028 by 2030, has intensified land development and impervious surface expansion, amplifying the UHI effect [26,14]. Areas with sparse or abandoned vegetation and bare soil have shown the strongest LST increases, consistent with global findings linking land cover degradation to surface warming [28, 29].

This rising trend in Siddharthanagar is consistent with broader regional and global patterns. Globally, annual average LST increased between 2003 and 2017, with the strongest gains observed north of 45°N (Liu et al., 2020). In North America, LST rose by approximately 0.07°C per year between 2002 and 2018 [30], while European cities such as Reykjavik experienced an increase of 7.7°C over several decades [31]. In South Asia, comparable urbanizing cities show similarly pronounced trends: Chittagong recorded a ~2°C rise over 30 years [28], Dhaka saw a 2.48°C increase in maximum LST in developed areas from 1988 to 2018 [32], and summer LST maxima in Indian semi-arid regions reached as high as 62°C between 2002 and 2022 [33].

The rate of increase observed in Siddharthanagar (0.18°C/year) is notably higher than the North American average, reflecting the compounding pressures of rapid urbanization and limited vegetation in the Tarai lowland context.

Driving factors for the rise of LST over the years

The increasing LST in Siddharthanagar is driven by a combination of climatic, biophysical, and anthropogenic

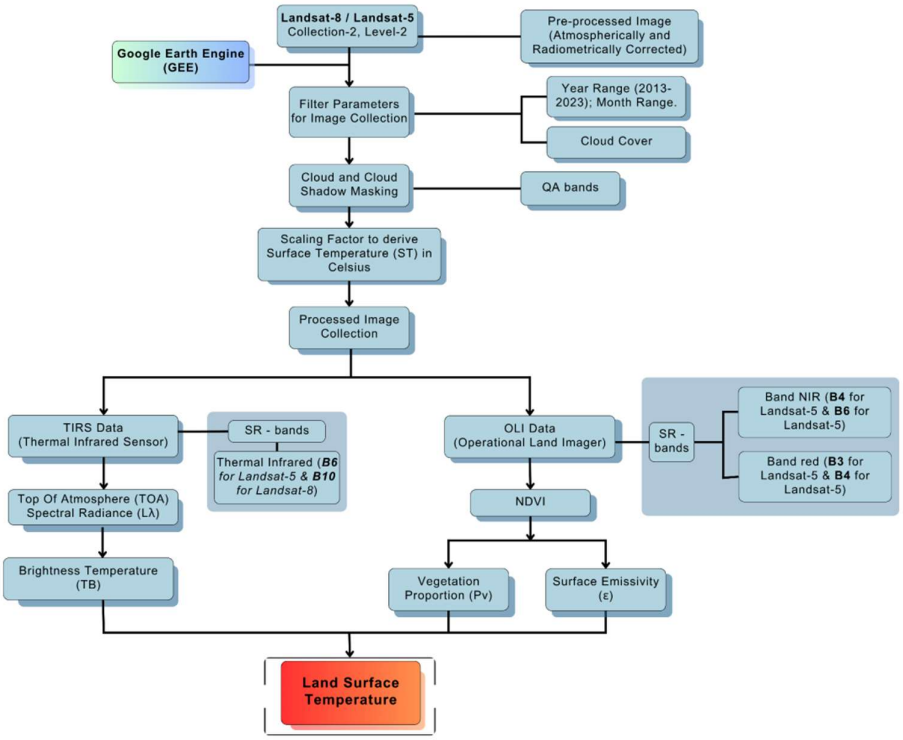

Figure 3: Flowchart of methods to extract LST.

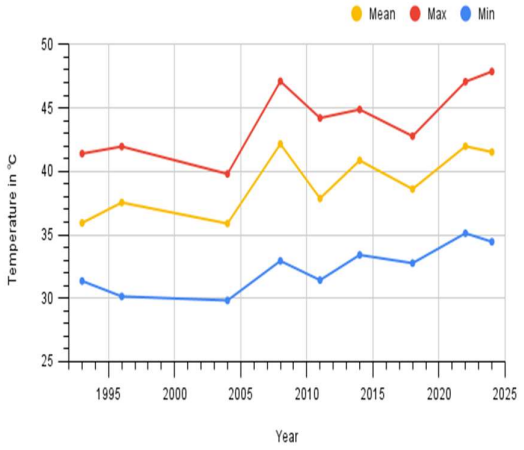

Figure 4: Temporal trend of LST from 1993-2024.

factors. Among biophysical factors, vegetation cover plays the most decisive role. The NDVI map of 2024 (Figure 9) clearly illustrates this relationship: wards with relatively higher NDVI values, particularly in parts of Ward 1 and pockets of the central wards, correspond spatially to areas of lower LST, while areas with low NDVI notably the border of Wards 4 and 10, characterized by the airport's impervious surface and surrounding bare ground display the highest LST values in the municipality. This spatial correspondence directly supports the well-established negateve correlation between NDVI and LST, whereby declining vegetation increases heat absorption and reduces evapotranspiration, elevating surface temperatures [18,28]. Urbanization, which replaces permeable vegetated surfaces with impervious built-up areas, further compounds this by reducing latent heat flux and increasing sensible heat, forming pronounced hotspots. The interplay of these climate, biophysical, and anthropogenic factors is examined in greater spatial detail in the following sections.

2. Spatial Pattern of LST

Significant spatial variability in LST across the study area is evident in Figure 5, with distinct patterns observed between years. Ward boundaries are labelled numerically to identify areas most affected by temperature change.

In 1993 (Figure 5a), LST was relatively moderate, with cooler areas concentrated in the central and southern wards (5, 12, 13, and 1), where temperatures did not exceed

41.4°C. By 1996 (Figure 5b), slight warming was observed in the northwestern wards (1, 4, and 5), while central and southern regions remained cooler. A notable cooling period occurred in 2004 (Figure 5c), with maximum temperatures falling to 39.8°C across central wards. By 2008 (Figure 5d), a dramatic rise in LST is recorded, with northern and central wards (1, 4, 5, and 6) peaking at 47.1°C marking one of the most extreme heat events in the study period. A slight moderation followed in 2011 (Figure 5e), though northern wards continued to exhibit elevated LST. In 2014 (Figure 5f), widespread warming returned, particularly across wards 1, 4, 10, and 11, reaching nearly 44.88°C. The 2018 map (Figure 5g) shows a minor cooling in central wards, while 2022 (Figure 5h) represents one of the hottest periods recorded, with temperatures exceeding 47°C in the northern and central wards (1, 4, 5, and 7), and even the typically cooler southern wards exhibiting noticeable warming.

Wards 2, 3, 4, 5, 10, and 11 consistently record the highest LST values across multiple years, identifying them as persistent heat stress zones. Historical imagery from Google Earth Pro confirms these areas were predominantly agricultural land that has progressively been converted or left bare during the dry season. The study window of March to May coincides with the dry pre-monsoon period, during which wet-season cultivation has ended and irrigation for dry-season farming is limited, leaving large areas as bare ground with high heat absorption [34].

This seasonal land condition substantially amplifies the LST signal captured in the analysis. Data from the results indicates a significant LST rise from 2008 onwards, with extreme temperatures becoming increasingly frequent by 2022. The 2009 satellite image of Ward 10 (Figure 6a) shows predominantly agricultural land, while the 2023 image (Figure 6b) reveals considerable expansion of the GBIA runway and associated impervious surfaces. This land cover change directly explains the sharp LST hotspot emerging along the border of Wards 10 and 4 in the later maps, where distinct hotspots visible in 2022 replace the more spatially diffuse high-temperature pattern observed in 2008.

In contrast, central wards (5, 6, 7, 8, 12, and 13) have generally maintained relatively lower temperatures despite being primarily built-up areas. This can be attributed to the presence of Pocket Green Spaces (PGS) in these urban areas, as shown in Figure 7. Figure 7 includes images from a selected urban area from the central wards in 2016 and 2023, where only slight changes in the green spaces are noticeable in certain areas. These PGS have played a key role in cooling the surrounding areas. A similar phenomenon has been observed during heat wave episodes in Mediterranean cities, where traditional squares, pocket parks, gardens, and pedestrian areas with trees and impervious surfaces have been more effective in reducing the likelihood of exceeding LST values above 41°C, compared to other vegetated patches mainly covered by herbaceous vegetation and grass [35].

3. Spatial Pattern of LST and NDVI in 2024

The year 2024 recorded the highest LST of the entire study period, with values ranging from 29.82°C to 47.87°C (Figure 8). Wards 4 and 10 stand out as the most intense heat zones, displaying extensive areas of elevated surface temperature, while the central wards remain comparatively cooler. Simultaneously, the NDVI map for 2024 (Figure 9) reveals a clear spatial correspondence: NDVI values range from -0.069 to 0.709, with the western parts of Ward 1 showing relatively healthy vegetation and the border of Wards 4 and 10 dominated by the airport's impervious surfaces and surrounding bare ground exhibiting the lowest NDVI values in the municipality.

The spatial overlap between low NDVI and high LST is particularly pronounced in Wards 4 and 10, where the absence of vegetation results in greater solar radiation absorption and reduced evaporative cooling, producing the most severe thermal hotspots. Conversely, areas in the southern part of Ward 1 near the boundary with Ward 2 show relatively higher NDVI values alongside lower LST, demonstrating the cooling effect of even modest vegetation in an otherwise heat-stressed landscape. In the central wards (5, 6, 7, 8, 12, and 13), small patches of higher NDVI corresponding to Pocket Green Spaces help moderate LST despite the predominantly built-up character of these wards.

These findings reinforce the inverse relationship between NDVI and LST documented across similar contexts. In West Bengal, strong negative correlations between NDVI and LST were observed from 2011 to 2020 [18].

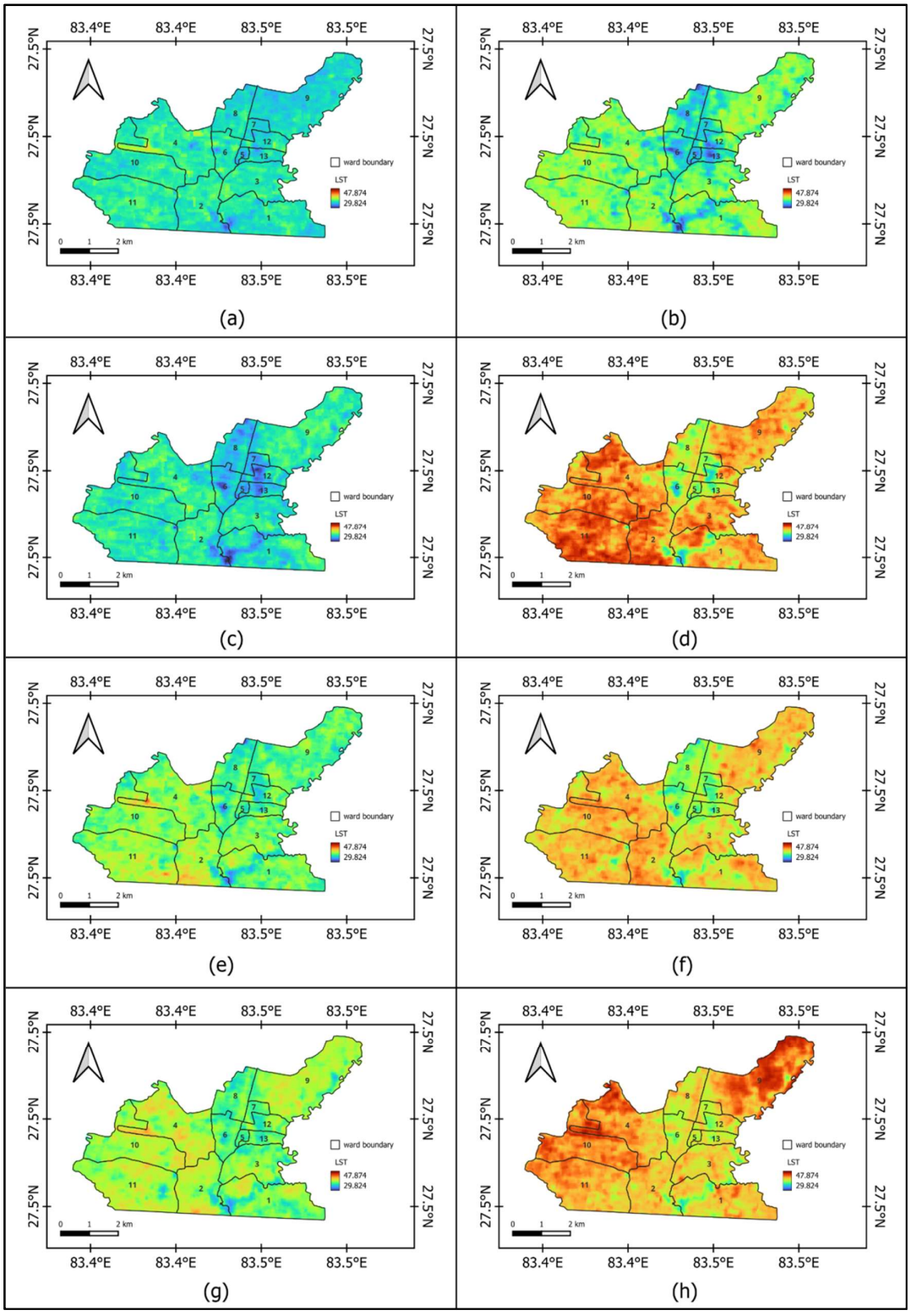

Figure 5: LST map of Siddharthanagar for years (a) 1993, (b) 1996, (c) 2004, (d) 2008, (e) 2011, (f) 2014, (g) 2018, and (h) 2022.

Figure 6: Satellite images from Google Earth Pro of the area near GBIA from (a) 2009 and (b) 2023.

Figure 7: Satellite images from Google Earth Pro of an urban area in central wards from the year (a) 2009 (b) 2023.

In Sylhet Sadar Upazila, Bangladesh, a significant negative correlation of -0.98 was recorded between NDVI and LST in vegetated areas [36]. In Dhaka, 30 years of data showed LST rising as urban NDVI fluctuated downward, underscoring the cooling role of vegetation amid intensifying urbanization

4. Relationship between LULC and LST

The analysis of LST with LULC reveals that areas with more vegetation tend to have lower surface temperatures, highlighting the critical role of greenery in cooling urban landscapes. For instance, areas dominated by trees, particularly in patches of Wards 1, 2, and 3 exhibit significantly lower LST values. Conversely, rangeland areas, which are characterized by sparse vegetation and degraded land cover, show higher LST values. This is evident in Wards 4, and 10, where large expanses of rangeland experience elevated temperatures. The lack of dense vegetation in these areas allows for more solar radiation absorption and less heat dissipation, contributing

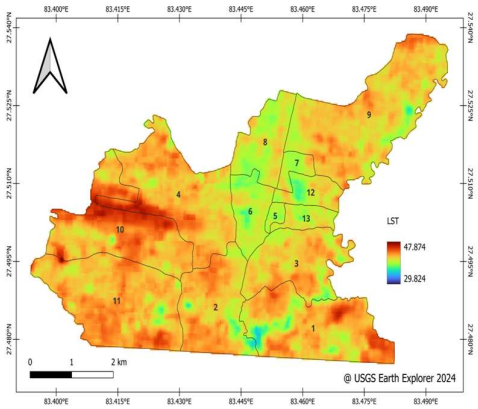

Figure 8: LST map of Siddharthanagar in 2024.

to the higher surface temperatures observed. During the study time, the land was largely bare ground, which had a higher heat absorption rate compared to vegetated areas, resulting in elevated LST. Bare ground, particularly in dry seasons, lacks the cooling effect provided by crops, leading to higher surface temperatures.

This phenomenon is evident in various case studies around the world. For instance, in the Barapukuria coal mining

region of Bangladesh, bare land showed the highest LST values, with a notable increase of 1.47°C. This temperature rise was closely linked with the conversion of agricultural land into bare soil and settlements, emphasizing the role of LULC changes in influencing LST [37]. Similarly, a study conducted in Colombo, Sri Lanka, found that both urban areas and bare land exhibited higher temperatures when compared to water bodies and vegetated areas. The ongoing development activities on bare land, coupled with reduced vegetation, contributed significantly to the elevated LST values in these areas [39].

Likewise, on Penang Island, Malaysia, a considerable expansion of urban and bare land between 2010 and 2021 led to a noticeable increase in LST. The loss of green areas, particularly agricultural lands, has further contributed to the warming effect, showcasing the direct link between reduced vegetation and increased surface temperatures [38]. In Vietnam's Bac Binh district, over a 30-year, the share of bare land increased dramatically, while green vegetation cover declined. This shift resulted in a significant increase in areas with LST values exceeding 35°C, demonstrating the clear relationship between land-cover change and rising temperatures [39]. This analysis reinforces the link between land cover types and their thermal properties, underscoring the importance of maintaining vegetated areas to mitigate urban heat and the potential heat risks posed by bare or degraded land covers.

5. NDVI Map of 2024

The NDVI map of 2024 provides a measure of vegetation health, with values ranging from -0.069423 to 0.708685 as shown in Figure 9. Higher NDVI values, seen in shades of darker green, represent healthier and denser vegetation, while lower values, in lighter shades, indicate sparse or degraded vegetation. Western parts of Wards 1 show relatively high NDVI values. In contrast, the southern part of Ward 1 and Ward 2 demonstrate lower NDVI values. In the central parts of the study area, wards 5, 6, 7, 8, 12, and 13, some areas have lower NDVI values, including small patches with higher NDVI values.

The unexpectedly lower LST values in certain built-up

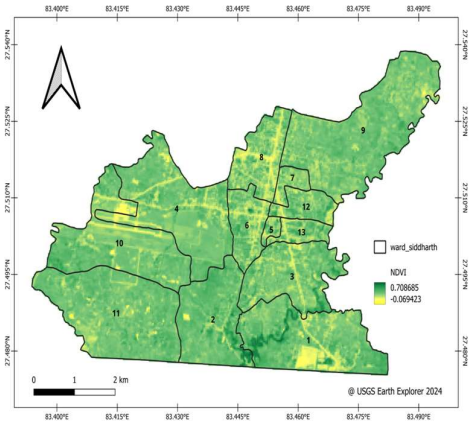

Figure 9: NDVI Map of Siddharthanagar in 2024.

areas, as seen in central wards, contrast with the typical trend of higher temperatures in urban zones. This is explained by the presence of PGS of urban vegetation, as shown in the NDVI map in Figure 9. A region in the southern part of Ward 1, near the border with Ward 2, also shows higher NDVI values accompanied by lower LST, demonstrating the significant cooling role of vegetation in these regions. In contrast, areas with lower NDVI values, indicating sparse vegetation, correspond to higher surface temperatures, particularly in the border of Wards 10 and 4, which are characterized by the impervious surface of the airport and bare ground. This result indicates the inverse correlation between LST and NDVI.

These findings are consistent with case studies from other regions. For example, in West Bengal, a study from 2011 to 2020 showed strong negative correlations between NDVI and LST, with higher vegetation associated with lower temperatures [18]. Similarly, in Sylhet Sadar Upazila, Bangladesh, the relationship between LST and various spectral indices revealed a significant negative correlation (-0.98) between NDVI and LST, particularly in areas with dense vegetation such as forests and wetlands. As NDVI increased, LST values dropped [36]. Further support comes from research conducted in Dhaka which observed a clear inverse relationship between NDVI and LST over 30 years. As urbanization intensified, LST rose while NDVI fluctuated, underscoring the cooling effect of vegetation and the impact of land cover changes on temperature [32]. These studies emphasize the vital role of vegetation in

mitigating urban heat, highlighting the need to preserve and enhance green spaces in urban areas to control LST.

6. Long-term solution to lower LST

To effectively lower LST in the long term, experts recommend a combination of strategies focused on increasing vegetation, optimizing urban design, incorporating cool surfaces, and improving overall urban planning [40]. One of the most impactful approaches is increasing vegetation cover. Increasing urban greenery can significantly reduce LST through shading and evapotranspiration. Optimizing the arrangement of buildings, landscapes, and roads to enhance the cooling benefits of vegetation is crucial. Additionally, increasing the diversity and density of urban forests can help lower temperatures in suburban areas [41]. For example, a study done in 193 European cities revealed that urban trees consistently exhibit lower LST. In Southern Europe, LSTs for urban trees up to 4°C lower, while in Central Europe, they are 8-12°C lower. Treeless green spaces are less effective, with a cooling effect that is 2-4 times weaker than that of urban trees [42].

Incorporating cool surfaces is also an effective strategy.

Using building materials with high albedo (reflectivity) reduces surface temperatures by reflecting more solar radiation. Cool roofs and pavements, which have higher albedo compared to traditional materials, can significantly mitigate the UHI effect. Increasing the reflectivity of urban surfaces is one of the most efficient ways to reduce LST [40]. In Covina, California, introducing cool pavement which increases pavement reflectivity lowered LST to a maximum of 5°C [43].

Finally, improving urban planning and design plays a crucial role. Buildings designed with passive cooling in mind remain cooler and help lower energy costs. A study by Rijal et al., (2018) found that traditional houses in Nepal, built with earthen floors, thatched roofs, and mud or brick walls, are effective at keeping indoor air temperatures lower. Cross ventilation, allowing wind to flow through a home for cooling, is another key technique [45]. Incorporating green infrastructure such as parks, gardens, and green roofs into urban spaces helps lower temperatures. Preserving existing green areas and creating new ones is essential for reducing urban heat. Incorporating water bodies like ponds and fountains adds additional cooling through evaporation while orienting streets and buildings to maximize natural ventilation can further enhance cooling [40].

Overall, a holistic approach combining vegetation, urban form optimization, cool materials, and thoughtful urban planning is necessary to effectively lower LST over time. Experts also emphasize the importance of tailoring these strategies to local climate conditions for maximum effectiveness.

Conclusion

This study analysed the temporal and spatial trends of LST in Siddharthanagar from 1993 to 2024 using GIS and remote sensing, revealing a clear upward trend with an average annual increase of 0.18°C and a peak temperature of 47.87°C recorded in 2024. The findings confirm that LULC change and declining vegetation cover are the primary drivers of rising LST. Areas with higher NDVI values, particularly vegetated patches in Wards 1, 2, and 3, consistently recorded lower surface temperatures, while areas dominated by bare ground and impervious surfaces most notably the border of Wards 4 and 10 experienced the highest LST values. Notably, certain central built-up wards maintained relatively cooler temperatures owing to the presence of Pocket Green Spaces, underscoring the cooling value of even small urban vegetation patches. The study highlights the urgent need for climate-adaptive urban planning in Siddharthanagar, including the expansion of green spaces, protection of agricultural land, and adoption of reflective surface materials to mitigate the UHI effect. Future research should prioritize ground-based validation of satellite-derived LST, investigation of diurnal temperature variations, and assessment of the socio-economic impacts of rising surface temperatures, to support more effective and resilient urban policy in the region.

Data Availability Statement

The Landsat-5 Thematic Mapper (TM) and Landsat-8 Operational Land Imager (OLI)/TIRS satellite imagery

used for Land Surface Temperature retrieval in this study are publicly available through the United States Geological Survey (USGS) Earth Explorer portal, accessible at https://earthexplorer.usgs.gov. The LULC data for 2023 were sourced from the ESRI Living Atlas of the World (https://livingatlas.arcgis.com). All satellite data processing, including LST retrieval, NDVI computation, and cloud masking, was performed using the Google Earth Engine (GEE) cloud computing platform (https://earthengin-e.google.com), which provides open access to the full Landsat archive.

Acknowledgements

I would like to express my sincere gratitude to Naaya Aayam Multi-Disciplinary Institute (NAMI) for providing me the opportunity to carry out this work as my dissertation.

References

1. Abdullah, S., Barua, D., Abdullah, S. M. A. & Rabby, Y. W. 2022. Investigating the impact of land use/land cover change on present and future land surface temperature (LST) of Chittagong, Bangladesh. *Earth Systems and Environment*. **6**(1): 221–235. Doi: https://doi.org/10.1007/s41748-021-00291-w.
2. Hulley, G. C., Ghent, D., Göttsche, F. M., Guillevic, P. C., Mildrexler, D. J. & Coll, C. 2019. Land surface temperature. *Taking the Temperature of the Earth*. **57**–127. Doi: 10.1016/B978-0-12-814458-9.00003-4.
3. Li, Z. L., Wu, H., Duan, S. B., Zhao, W., Ren, H., Liu, X., Leng, P., Tang, R., Ye, X., Zhu, J. & Sun, Y. 2023. Satellite remote sensing of global land surface temperature: definition, methods, products, and applications. *Reviews of Geophysics*. **61**(1). Doi: https://doi.org/10.1029/2022RG000777.
4. Wang, M., Zhang, Z., Hu, T., Wang, G., He, G., Zhang, Z., Li, H., Wu, Z. & Liu, X. 2020. An efficient framework for producing Landsat-based land surface temperature data using Google Earth Engine. *IEEE Journal of Selected Topics in Applied Earth Observations and Remote Sensing*. **13**: 4689–4701. Doi: 10.1109/JSTARS.2020.3014586.
5. Ma, Q., Wu, J. & He, C. 2016. A hierarchical analysis of the relationship between urban impervious surfaces and land surface temperatures: Spatial scale dependence, temporal variations, and bioclimatic modulation. *Landscape Ecology*. **31**: 1139–1153. Doi: https://doi.org/10.1007/s10980-016-0356-z.
6. Chen, Y. C., Chiu, H. W., Su, Y. F., Wu, Y. C. & Cheng, K. S. 2017. Does urbanization increase diurnal land surface temperature variation? Evidence and implications. *Landscape and Urban Planning*. **157**: 247–258. Doi: https://doi.org/10.1016/j.landurbplan.2016.06.014.
7. Thapa, S. 2017. *Exploring the impact of urban growth on land surface temperature of Kathmandu Valley, Nepal*. Dissertation. Universitat Jaume I, Castellón, Spain.
8. Sahana, M., Dutta, S. & Sajjad, H. 2019. Assessing land transformation and its relation with land surface temperature in Mumbai city, India using geospatial techniques. *International Journal of Urban Sciences*. **23**(2): 21. Doi: https://doi.org/10.1080/12265934.2018.1488604.
9. Fonseka, H., Zhang, H., Sun, Y., Su, H., Lin, H. & Lin, Y. 2019. Urbanization and its impacts on land surface temperature in Colombo Metropolitan Area, Sri Lanka, from 1988 to 2016. *Remote Sensing*. **11**(8): 957. Doi: https://doi.org/10.3390/rs11080957.
10. Yang, J., Ren, J., Sun, D., Xiao, X., Xia, J., Jin, C. & Li, X. 2021. Understanding land surface temperature impact factors based on local climate zones. *Sustainable Cities and Society*. **69**: 10. Doi: https://doi.org/10.1016/j.scs.2021.102818.
11. Hassan, T., Zhang, J., Prodhan, F. A., Pangali Sharma, T. P. & Bashir, B. 2021. Surface urban heat islands dynamics in response to LULC and vegetation across South Asia (2000–2019). *Remote Sensing*. **13**(16): 3177. Doi: https://doi.org/10.3390/rs13163177.
12. Islam, M. Y., Mohiuddin, M., Hossain, K. T., Salauddin, M. & Farin, S. 2024. Trend of heat waves in Dhaka Metropolitan City and its impact on livelihood and health of exposed people. *Arabian Journal of Geosciences*. **17**(8). Doi: https://doi.org/10.1007/s12517-024-12027-x.
13. Poudel, A. 2024, April 26. Sweltering heat causes distress across Tarai. *The Kathmandu Post*. https://kathmandupost.com/national-/2024/04/26/sweltering-heat-causes-distress-across-tarai-17140957-96.
14. Ministry of Urban Development. 2017. *National Urban Development Strategy (NUDS) 2017 Part B.* Government of Nepal.
15. Rimal, B., Sloan, S., Keshtkar, H., Sharma, R., Rijal, S. & Shrestha, U. B. 2020. Patterns of historical and future urban expansion in Nepal. *Remote Sensing*. **12**(4): 22. Doi: https://doi.org/10.3390/rs12040628.
16. Bhattarai, K., Adhikari, A. P. & Gautam, S. P. 2023. State of urbanization in Nepal: The official definition and reality. *Environmental Challenges*. **13**: 100776. Doi: https://doi.org/10.1016/j.envc.2023.100776.
17. Subedi, P., Ojha, P., Adhikari, A., Acharya, S. & Acharya, S. 2022. Mapping of major land use land cover dynamics and its driving factors: A case study of Nepalgunj Sub-Metropolitan City, Banke, Nepal. *Indonesian Journal of Social and Environmental Issues (IJSEI)*. **3**(1), 67–80. Doi: https://doi.org/10.47540/ijsei.v3i1.468.
18. Garai, S., Khatun, M., Singh, R., Sharma, J., Pradhan, M., Ranjan, A., Rahaman, S. M., Khan, M. L. & Tiwari, S. 2022. Assessing correlation between rainfall, normalized difference vegetation index

(NDVI) and land surface temperature (LST) in Eastern India. *Safety in Extreme Environments*. **4**(2): 119–127.
Doi: https://doi.org/10.1007/s42797-022-00056-2.

19. Yu, Z., Guo, X., Zeng, Y., Koga, M. & Vejre, H. 2018. Variations in land surface temperature and cooling efficiency of green space in rapid urbanization: The case of Fuzhou City, China. *Urban Forestry and Urban Greening*. **29**: 113–121.
Doi: https://doi.org/10.1016/j.ufug.2017.11.008.
20. National Statistics Office. 2001. National population and housing census 2001. Census Nepal.
21. National Statistics Office. 2021. National population and housing census 2021. https://censusnepal.cbs.gov.np
22. Office of the Municipal Executive. 2021. Municipality Transport Master Plan (MTMP) of Siddharthanagar Municipality. RIDARC Nepal Pvt. Ltd.
23. Reiners, P., Sobrino, J. & Kuenzer, C. 2023. Satellite-derived land surface temperature dynamics in the context of global change-
A review. *Remote Sensing*. **15**(7).
Doi: https://doi.org/10.3390/rs15071857
24. Kanauje, N. 2023. *Gastrointestinal parasites of quail in Siddharthanagar, Rupandehi, Nepal. Doctoral Dissertation.* Central Department of Zoology.
25. Khanal, B. R. 2020. Assessing the environmental impacts of urbanization in Siddharthanagar, Nepal. University of New Mexico MLA.
https://digitalrepository.unm.edu/econ_etds/113
26. Siddharthanagar Municipality. 2024. Brief introduction. https://siddharthanagarmun.gov.np/en/node/40
27. Waleed, M. and Sajjad, M., 2022. Leveraging cloud-based computing and spatial modeling approaches for land surface temperature disparities in response to land cover change: evidence from Pakistan. *Remote Sensing Applications: Society and Environment*. **25**.
Doi: https://doi.org/10.1016/j.rsase.2021.100665.
28. Abdullah, S., Barua, D., Abdullah, S. M. A. & Rabby, Y. W. 2022. Investigating the impact of land use/land cover change on present and future land surface temperature (LST) of Chittagong, Bangladesh. *Earth Systems and Environment*. **6**(1): 221–235.
Doi: https://doi.org/10.1007/s41748-021-00291-w.
29. Liu, J., Hagan, D. F. T. & Liu, Y. 2020. Global land surface temperature change 2003–2017 and its relationship with climate drivers: AIRS, MODIS, and ERA5-land based analysis. *Remote Sensing*. **13**(1): 44.
Doi: https://doi.org/10.3390/rs13010044.
30. Yan, Y., Mao, K., Shi, J., Piao, S., Shen, X., Dozier, J., Liu, Y., Ren, H. L. & Bao, Q. 2020. Driving forces of land surface temperature anomalous changes in North America in 2002–2018. *Scientific Reports*. **10**(1): 6931.
Doi: https://doi.org/10.1038/s41598-020-63701-5.
31. Mansourmoghaddam, M., Rousta, I., Zamani, M. & Olafsson, H. 2023. Investigating and predicting land surface temperature (LST) based on remotely sensed data during 1987–2030 (A case study of Reykjavik city, Iceland). *Urban Ecosystems*. **26**(2): 337–359.
Doi: https://doi.org/10.1007/s11252-023-01337-9.
32. Begum, M. S., Bala, S. K., Islam, A. S., Islam, G. T. & Roy, D. 2021. An analysis of spatio-temporal trends of land surface temperature in the Dhaka metropolitan area by applying Landsat images. *Journal of Geographic Information System*. **13**(4): 538–560.
Doi: 10.4236/jgis.2026.182007.
33. Pandey, P. C., Chauhan, A. & Maurya, N. K. 2022. Evaluation of earth observation datasets for LST trends over India and its implication in global warming. *Ecological Informatics*. **72**: 101843.
Doi: https://doi.org/10.1016/j.ecoinf.2022.101843.
34. Jacoby, H. G. & Walker, T. 2019. The monsoon shock in rural Nepal: panel evidence from the household risk and vulnerability survey. *The World Bank*. 1-29.
35. Delgado-Capel, M. J., Egea-Cariñanos, P. & Cariñanos, P. 2024. Assessing the relationship between land surface temperature and composition elements of urban green spaces during heat waves episodes in Mediterranean cities. *Forests*. **15**(3).
Doi: https://doi.org/10.3390/f15030463.
36. Roy, B. & Bari, E. 2022. Examining the relationship between land surface temperature and landscape features using spectral indices with Google Earth Engine. *Heliyon*. **8**(9).
Doi: 10.1016/j.heliyon.2022.e10668
37. Tabassum, A., Basak, R., Shao, W., Haque, M. M., Chowdhury, T. A. and Dey, H. 2023. Exploring the relationship between land use land cover and land surface temperature: a case study in Bangladesh and the policy implications for the Global South. *Journal of geovisualization and spatial analysis*. **7**(2).
Doi: https://doi.org/10.1007/s41651-023-00155-z.
38. Akomolafe, G. F. & Rosazlina, R. 2022. Land use and land cover changes influence the land surface temperature and vegetation in Penang Island, Peninsular Malaysia. *Scientific Reports*. **12**(1): 21250.
Doi: https://doi.org/10.1038/s41598-022-25560-0.
39. Dang, T., Yue, P., Bachofer, F., Wang, M. and Zhang, M. 2020. Monitoring land surface temperature change with landsat images during dry seasons in Bac Binh, Vietnam. *Remote Sensing*. **12**(24).
Doi: https://doi.org/10.3390/rs12244067.
40. Singh, R. & Subedi, A. 2022. Reducing heat impacts in Nepalgunj City, Nepal (Policy Brief). Red Cross Red Crescent Climate Centre.
41. Wang, Z., Ishida, Y. & Mochida, A. 2023. Effective factors for reducing land surface temperature in each local climate zone-built type in Tokyo and Shanghai. *Remote Sensing*. **15**(15): 3840.
Doi: https://doi.org/10.3390/rs15153840.
42. Schwaab, J., Meier, R., Mussetti, G., Seneviratne, S., Bürgi, C. & Davin, E. L. 2021. The role of urban trees in reducing land surface temperatures in European cities. *Nature Communications*. **12**(1).
Doi: https://doi.org/10.1038/s41467-021-26768-w.
43. Ko, J., Schlaerth, H., Bruce, A., Sanders, K. and Ban-Weiss, G. 2022. Measuring the impacts of a real-world neighborhood-scale cool pavement deployment on albedo and temperatures in Los Angeles.

Environmental Research Letters. **17**(4):.044027.
Doi: 10.1088/1748-9326/ac58a8.

44. Rijal, H. B. 2018. Passive cooling of the traditional houses of Nepal. *Sustainable Houses and Living in the Hot-Humid Climates of Asia*. **397**-406.
Doi: https://doi.org/10.1007/978-981-10-8465-2_38

45. Bhatta, K. and Pahari, S. 2021. Vulnerability to heat stress and its health effects among people of Nepalgunj Sub-Metropolitan. *Journal of Nepal Health Research Council*. **18**(4): 763-768.
Doi: https://doi.org/10.33314/jnhrc.v18i4.2734.